Mass Effect in Single Flavor Color Superconductivity

Ping-ping Wu,[1,2,*] De-fu Hou,[1,†] and Hai-cang Ren[1,3,‡]

[1] *Institute of Particle Physics, Huazhong Normal University, Wuhan, 430079, China*
[2] *The Key Laboratory of Quark and Lepton Physics(HZNU), Ministry of Education, Wuhan 430079, China*
[3] *Physics Department, The Rockefeller University, 1230 York Avenue, New York, NY 10021-6399*

The nonzero strange quark mass effect in different types of single flavor color superconductivity and the phase diagram in a magnetic field are studied. We have obtained simple analytical forms of the quasi-particle energies for an arbitrary mass and explored the mass correction to the pressure and the transition temperature. It is found that the mass reduces the pressure and transition temperature of strange quarks, but it doesn't change the ranking $P_n < P_{\rm A} < P_{\rm polar} < P_{\rm planar} < P_{\rm CSL}$ of the pressure for the four canonical single flavor phases. The phase diagram with magnetic field and temperature for a system of three flavors is obtained for two different values of the strange quark mass. The changes from the one obtained previously under the approximation of massless strange quarks are examined.

PACS numbers: 12.38.Aw, 11.15.Ex, 24.85.+p

1. INTRODUCTION

Quark matter at sufficiently high baryon density and low temperature becomes a color superconductor(CSC) [1]. CSC is characterized by a diquark condensate, which is analogous to the Cooper pair in an ordinary superconductor, but the structure of the condensate is much richer because quarks have the nonabelian color and flavor charges.

The structure of the CSC states depends sensitively on the number of quark flavors and their masses [2–5]. For very high baryon density, where the masses of u, d and s quarks can be ignored, the ground state is in the color-flavor-locked(CFL) phase [6], where quarks of different flavors pair. The situation becomes more complicated in moderate density because of the strange quark mass, β equilibrium and the charge neutrality conditions. A substantial Fermi momentum mismatch among different quark flavors is introduced and thereby reduces the available phase space for the cross-flavor pairing, such as CFL. Different exotic scenarios for cross-flavor pairing proposed in the literature (gapless CSC, LOFF CSC etc.) either run into various instabilities [7–9] or reduce significantly the condensation energy. This makes the single flavor pairing, which is free from the Fermi momentum mismatch and the instabilities, a competing alternative even though the pairing force here is expected to be weaker. There are a number of different paring states. The ones frequently discussed in the literature include the spherical color-spin-lock(CSL) and nonspherical planar, polar and A [10–12]. Here, the adjective "spherical/nonspherical" refers to the symmetry of the order parameter under a space rotation. The CSL pairing is energetically most favored in the absence of a magnetic field, but the situation changed when a magnetic field is applied. The single flavor color superconductivity may be realized in the interior of a compact star during the later stage of its life, where a magnetic field is present.

The presence of a magnetic field in the interior of a compact star [13] will offset the energy balance among the four canonical single flavor pairings. The spherical CSL phase has an electromagnetic Meissner effect [11], but nonspherical phases: polar, A and planar phases do not. So if a quark matter of single flavor parings cools down through the critical temperature in a magnetic filed, forming CSL state will cost extra work to exclude magnetic fluxes from the bulk. Therefore, the magnetic contribution to the free energy may favor the nonspherical states. In a previous work, we have explored the consequences of the absence of the electromagnetic Meissner effect in a nonspherical CSC phase of single flavor pairing [14] and have obtained the phase diagram with respect to the magnetic field and the temperature. We found that under the plausible magnitude of the the magnetic field inside a compact star, the most favored state is not always CSL and nonspherical pairing states may show up. For the sake of simplicity, we considered both the infinitely massive limit and the massless limit strange quarks in [14]. The former limit is unrealistic given the typical chemical potential μ around 500MeV, the latter requires the mass of strange quarks, m_s, to be much lower than quark chemical potential. On the other hand, m_s has to be sufficiently large in order to win the competition with exotic cross-flavor pairings such as gapless CSC and LOFF. Both requirements may be compromised marginally for the value

*Electronic address: wupingping@iopp. ccnu. edu. cn
†Electronic address: hdf@iopp. ccnu. edu. cn
‡Electronic address: ren@mail.rockefeller.edu

of m_s in vacuum ($\sim$ 150MeV) but will be problematic when the value of m_s in medium becomes comparable with μ as was suggested by some numerical works such as [15]. All these concerns warrant a systematic treatment of the single flavor pairing with an arbitrary quark mass. So we did in this paper.

In the present work, we shall give a detailed investigation of the phase structure. For this purpose, we formulate the single flavor CSC for an nonzero quark mass in terms of the same NJL(Nambu-Jona-Lasinio)-like effective action employed in [14] and introduce the mean-field approximation for an arbitrary mass in section 2. Unlike the ultra-relativistic limit, where the cross-helicity(transverse) pairing dominates, the nonzero quark mass couples the cross helicity pairing channel and the equal-helicity(longitudinal) pairing channel and thereby complicates the gap matrix underlying the excitation spectrum. Fortunately, as will be shown in section 3, the gap matrix for an arbitrary mass can still be diagonalized analytically for all four canonical phases and our results interpolate both the ultra-relativistic limit and the non-relativistic limit in the literature. The ranking of the condensation energy in the massless limit remains intact when a nonzero quark mass is switched on. In section 4 we generalize our analysis in [14] of a three-flavor quark matter beyond the ultra-relativistic limit. Because the transition temperature of the nonzero m_s strange quark paring is reduced, phase diagram with respect to temperature and magnetic field contains a region where only u and d flavors condensate. The size of this region is tiny for $m_s \sim 150$MeV but cannot be ignored for $m_s \sim \mu$. Finally, we summarize our results and remark on some open issues in section 5. Throughout the paper, we shall assume zero masses for u and d quarks as we did in [14]. All gamma matrices are hermitian according to our notation.

2. THE HAMILTONIAN UNDER MEAN FIELD APPROXIMATION

In this section and the next one, we shall formulate the single flavor Copper pairing with an arbitrary quark mass. The Lagrangian density of the NJL-like effective action reads [16]:

$$\mathcal{L} = \bar{\psi}(-\gamma_\nu \partial_\nu + m + \mu\gamma_4)\psi - G\bar{\psi}\gamma_\nu T^l \psi \bar{\psi}\gamma_\nu T^l \psi \tag{2.1}$$

where $T^l = \frac{1}{2}\lambda^l$ with λ^l the lth Gell-Mann matrix, m is the quark mass and μ is the chemical potential. We set the effective coupling $G > 0$, in accordance with the interaction mediated by one-gluon exchange at high density and that mediated by instantons for intermediate density. The corresponding Hamiltonian is

$$H = \int d^3\mathbf{r}\Big[\bar{\psi}(\gamma\cdot\nabla + m - \mu\gamma_4)\psi + G\bar{\psi}\gamma_\nu T^l\psi\bar{\psi}\gamma_\nu T^l\psi\Big] \tag{2.2}$$

Like QCD Lagrangian, the diquark scattering in (2.1) conserves the eigenvalues of γ_5 of each quark. At $m = 0$, the eigenvalue γ_5 coincides with the helicity so that the helicity of each quark is also conserved during the scattering. The process like

$$(R, R) \to (R, L) \tag{2.3}$$

with R(L) the right(left) hand helicity will never occur and the transverse pairing will not couple with the longitudinal one. For $m \neq 0$, however, the helicity is not the eigenvalue of γ_5 and is no longer conserved. The two types of pairing do couple via (2.3).

The thermodynamic pressure

$$P = \frac{T}{\Omega}\ln\exp\left(-\frac{H}{T}\right) \tag{2.4}$$

with T the temperature and Ω the volume of the system and the ensemble average of the operator O is given by

$$< O >= \frac{\mathrm{Tr}\left[\exp\left(-\frac{H}{T}\right)O\right]}{\mathrm{Tr}\left[\exp\left(-\frac{H}{T}\right)\right]} \tag{2.5}$$

In terms of the plane-wave expansion:

$$\psi = \frac{1}{\sqrt{\Omega}}\sum_{\mathbf{p},s}(a_{\mathbf{p},s}u_{\mathbf{p},s}e^{i\mathbf{pr}} + b^+_{\mathbf{p},s}v_{\mathbf{p},s}e^{-i\mathbf{pr}}) \tag{2.6}$$

with $s(=\pm\frac{1}{2})$ the helicity defined by

$$\sigma\cdot\mathbf{p}u_{\mathbf{p},s} = 2spu_{\mathbf{p},s} \qquad \sigma\cdot\mathbf{p}v_{\mathbf{p},s} = -2spv_{\mathbf{p},s} \tag{2.7}$$

the interaction Hamiltonian reads

$$\begin{aligned} H_{\rm int} &= G\bar{\psi}\gamma_\nu T^l\psi\bar{\psi}\gamma_\nu T^l\psi \\ &= \frac{1}{\Omega}\sum_{\mathbf{p},\mathbf{p}'} a^\dagger_{\mathbf{p}',s_1'} T^l a_{-\mathbf{p},s_2} a^\dagger_{-\mathbf{p}',s_2'} T^l a_{\mathbf{p},s_1} \bar{u}^\dagger_{\mathbf{p}',s_1'}\gamma_\nu u_{-\mathbf{p},s_2}\bar{u}^\dagger_{-\mathbf{p}',s_2'}\gamma_\nu u_{\mathbf{p},s_1} \\ &+ \text{ the terms containing antiquark operators, } b\text{'s} \end{aligned} \tag{2.8}$$

The formulae

$$T^l_{ij}T^l_{km} = -\frac{1}{3}(\delta_{ij}\delta_{km} - \delta_{im}\delta_{kj}) + \frac{1}{6}(\delta_{ij}\delta_{km} + \delta_{im}\delta_{kj}) \tag{2.9}$$

enables us to decompose the diquark interaction into color-antisymmetric and symmetric channels and the interaction within the former is attractive and therefore responsible for Cooper pairing for $G > 0$. We have

$$a^\dagger_{\mathbf{p}',s_1'} T^l a_{-\mathbf{p},s_2} a^\dagger_{-\mathbf{p}',s_2'} T^l a_{\mathbf{p},s_1} = \frac{1}{3} a^\dagger_{\mathbf{p}',s_1'}\varepsilon^c \tilde{a}^\dagger_{-\mathbf{p}',s_2'}\tilde{a}_{-\mathbf{p},s_2}\varepsilon^c a_{\mathbf{p},s_1} + \text{the color symmetric interaction} \tag{2.10}$$

where the 3×3 antisymmetric matrix ε^c in color space is defined by $(\varepsilon^1) = \lambda_5$, $(\varepsilon^2) = \lambda_7$ and $(\varepsilon^3) = \lambda_2$ and they coincide with the matrix representation of the angular momentum operators of spin one with respect to cartesian basis. We shall designate J_x, J_y and J_z for λ_5, λ_7 and λ_2 below. Furthermore, the gap energy associated to spin-one Cooper pairing is expected much smaller than the chemical potential. Therefore, we may drop the antiquark contribution and keep only the color antisymmetric interaction under the mean field approximation. The relevant Hamiltonian takes the form

$$H_{\rm eff} = \sum_{\mathbf{p},\mathbf{s}} v_F(p-k_F)a^+_{\mathbf{p}s}a_{\mathbf{p}s} - \frac{G}{3\Omega}\sum_{\mathbf{p},\mathbf{p}',\mathbf{s_1'},\mathbf{s_2'},\mathbf{s_1},\mathbf{s_2}} A_{s_1',s_2';s_1,s_2}(\mathbf{p}',\mathbf{p}) a^\dagger_{\mathbf{p}',s_1'}\varepsilon^c\tilde{a}^\dagger_{-\mathbf{p}',s_2'}\tilde{a}_{-\mathbf{p},s_2}\varepsilon^c a_{\mathbf{p},s_1} \tag{2.11}$$

where

$$A_{s_1',s_2';s_1,s_2}(\mathbf{p}',\mathbf{p}) \equiv u^\dagger_{\mathbf{p}',s_1'}\gamma_4\gamma_\nu u_{-\mathbf{p},s_2} u^\dagger_{-\mathbf{p}',s_2'}\gamma_4\gamma_\nu u_{\mathbf{p},s_1} \tag{2.12}$$

and the approximation $\sqrt{p^2+m^2}-\mu \simeq v_F(p-k_F)$ has been made with the Fermi momentum $k_F = \sqrt{\mu^2-m^2}$ and the Fermi velocity $v_F = k_F/\mu$.

To simplify (2.11) further, we employ the explicit form of the four component spinor in the chiral representation

$$u_{\mathbf{p},s} = \begin{pmatrix} \sqrt{\frac{E+2sp}{2E}}\phi_{\mathbf{p},s} \\ \sqrt{\frac{E-2sp}{2E}}\phi_{\mathbf{p},s} \end{pmatrix} \tag{2.13}$$

where the two component spinor ϕ given by

$$\phi_{\mathbf{p},\frac{1}{2}} = \begin{pmatrix} \cos\frac{\varphi}{2} \\ e^{i\varphi}\sin\frac{\theta}{2} \end{pmatrix} \qquad \phi_{\mathbf{p},-\frac{1}{2}} = \begin{pmatrix} -e^{-i\varphi}\sin\frac{\theta}{2} \\ \cos\frac{\theta}{2} \end{pmatrix} \tag{2.14}$$

with (θ,φ) the polar angles of $\mathbf{p}$. Our choice of the phases of $\phi_{\mathbf{p},\pm\frac{1}{2}}$ is to make them corresponding to the two columns of the standard Wigner D-matrix of the angular momentum $J = 1/2$, i. e.

$$\left(\ \phi_{\mathbf{p},\frac{1}{2}}, \phi_{\mathbf{p},-\frac{1}{2}}\ \right) = D^{\frac{1}{2}}(\varphi,\theta,-\varphi) \tag{2.15}$$

where

$$D^J_{m'm}(\alpha,\beta,\gamma) \equiv < Jm'|e^{-iJ_z\alpha}e^{-iJ_y\beta}e^{-iJ_z\gamma}|Jm > \tag{2.16}$$

with $\mathbf{J}$ the angular momentum operator and (α,β,γ) Euler angles. The chiral representation of gamma matrices is

$$\begin{pmatrix} 0 & \sigma_\nu \\ \bar{\sigma}_\nu & 0 \end{pmatrix} \tag{2.17}$$

where $\sigma_\nu = (1,\sigma), \bar{\sigma}_\nu = (1,-\sigma)$ with σ's the Pauli matrices.

After some algebra detailed in the appendix A, we find that

$$H_{\text{eff}} = \sum_{\mathbf{p},\mathbf{s}} v_F(p-k_F) a^+_{\mathbf{p}s} a_{\mathbf{p}s} - \frac{4G}{\Omega} \sum_{\mathbf{p},\mathbf{p}'}{}' \Phi^{\nu\dagger}_\mu(\mathbf{p}') \Phi^\nu_\mu(\mathbf{p}) \tag{2.18}$$

where

$$\Phi^\nu_\mu(\mathbf{p}) = \sum_{s_1,s_2} (-1)^{s_2-\frac{1}{2}} e^{-i\theta_{\mathbf{p}s_2}} B_{s_1 s_2}(p) \begin{pmatrix} \frac{1}{2} & \frac{1}{2} & 1 \\ -s_2 & s_1 & s_2 - s_1 \end{pmatrix} D^{1\,*}_{\mu,s_2-s_1}(\varphi,\theta,-\varphi) \tilde{a}_{-\mathbf{p}s_2} J^\nu a_{\mathbf{p}s_1} \tag{2.19}$$

with the phase $\theta_{\mathbf{p},s}$ is defined by the relation

$$e^{-i\theta_{\mathbf{p},s}} = -i(-1)^{s-\frac{1}{2}} \phi^\dagger_{\mathbf{p},-s} \phi_{-\mathbf{p},s} = ie^{2is\varphi} \tag{2.20}$$

and $B_{\frac{1}{2}\frac{1}{2}}(p) = B_{-\frac{1}{2}-\frac{1}{2}}(p) = \lambda = \frac{m}{E} \simeq \frac{m}{\mu}, B_{\frac{1}{2}-\frac{1}{2}}(p) = B_{-\frac{1}{2}\frac{1}{2}}(p) = 1$. The repeated indexes in the second term of (2.21) are summed over with $\mu,\nu = 0,\pm$ and the summation $\sum'_{\mathbf{p}}$ extends to half of the momentum space. We have defined $J_\pm \equiv (\varepsilon^1 \pm i\varepsilon^2)$ and $J_0 \equiv \varepsilon^3$ in (2.18).

Introducing a long range order $\langle \tilde{a}_{-\mathbf{p}s_2} \varepsilon^c a_{\mathbf{p}s_1} \rangle$ and expanding the interaction term of (2.19) to the linear order of the fluctuation $\tilde{a}_{-\mathbf{p}s_2} \varepsilon^c a_{\mathbf{p}s_1} - \langle \tilde{a}_{-\mathbf{p}s_2} \varepsilon^c a_{\mathbf{p}s_1} \rangle$, we obtain the linearized mean-field Hamiltonian

$$H_{\text{MF.}} = \sum_{\mathbf{p},\mathbf{s}} v_F(p-k_F) a^+_{\mathbf{p}s} a_{\mathbf{p}s} + \frac{9\Omega}{4G} \Delta^{\nu*}_\mu \Delta^\nu_\mu - 3 \sum_{\mathbf{p}} [\Delta^\nu_\mu \Phi^\nu_\mu(\mathbf{p}) + \Delta^{\nu*}_\mu \Phi^{\nu\dagger}_\mu(\mathbf{p})] \tag{2.21}$$

where the order parameter Δ^ν_μ is defined by

$$\frac{1}{\Omega} \sum_{\mathbf{p}} \langle \Phi^\nu_\mu(\mathbf{p}) \rangle^* = \frac{3\Delta^\nu_\mu}{4G} \tag{2.22}$$

and will be regarded the element of a 3×3 matrix with $\mu(\nu)$ the row(column) index. In terms of the Nambu-Gorkov basis

$$A^+_{\mathbf{p}} = \begin{pmatrix} e^{-i\theta_{\mathbf{p},\frac{1}{2}}} \tilde{a}_{-\mathbf{p},\frac{1}{2}} & e^{-i\theta_{\mathbf{p},-\frac{1}{2}}} \tilde{a}_{-\mathbf{p},-\frac{1}{2}} & -a^+_{\mathbf{p},-\frac{1}{2}} & a^+_{\mathbf{p},\frac{1}{2}} \end{pmatrix} \qquad A_{\mathbf{p}} = \begin{pmatrix} e^{i\theta_{\mathbf{p},\frac{1}{2}}} \tilde{a}^+_{-\mathbf{p},\frac{1}{2}} \\ e^{i\theta_{\mathbf{p},-\frac{1}{2}}} \tilde{a}^+_{-\mathbf{p},-\frac{1}{2}} \\ -a_{\mathbf{p},-\frac{1}{2}} \\ a_{\mathbf{p},\frac{1}{2}} \end{pmatrix} \tag{2.23}$$

the Hamiltonian (2.21) takes the form

$$H_{\text{MF.}} = \frac{9}{4G} \Delta^{\nu*}_\mu \Delta^\nu_\mu + \sum_{\mathbf{p}}{}' v_F(p-k_F) + \sum_{\mathbf{p}}{}' A^+_{\mathbf{p}} h_{\mathbf{p}} A_{\mathbf{p}} \tag{2.24}$$

where

$$h_{\mathbf{p}} = \begin{pmatrix} v_F(p-k_F) & M \\ M^\dagger & -v_F(p-k_F) \end{pmatrix} \tag{2.25}$$

and the 6×6 matrix M is defined by

$$M = \sqrt{3} \Delta^\nu_\mu J_\nu \times \begin{pmatrix} D^{1*}_{\mu,1}(\varphi,\theta,-\varphi) & \frac{\lambda}{\sqrt{2}} D^{1*}_{\mu,0}(\varphi,\theta,-\varphi) \\ \frac{\lambda}{\sqrt{2}} D^{1*}_{\mu,0}(\varphi,\theta,-\varphi) & D^{1*}_{\mu,-1}(\varphi,\theta,-\varphi) \end{pmatrix} \tag{2.26}$$

with $\times$ the direct product and $\lambda = \frac{m}{\mu}$. We have

$$h^2_{\mathbf{p}} = \begin{pmatrix} v^2_F(p-k_F)^2 + MM^\dagger & 0 \\ 0 & -v^2_F(p-k_F)^2 - M^\dagger M \end{pmatrix} \tag{2.27}$$

where both $MM^\dagger$ and $M^\dagger M$ have identical nonnegative eigenvalues, δ^2_n with $n = 1,...,6$ and the quasi-particle energy reads $E_{p,n} = \sqrt{v^2_F(p-k_F)^2 + \delta^2_n}$. Replacing the hamiltonian H of (2.4) by the linearized one of (2.21), we end up with the pressure under the mean-field approximation

$$P = -\frac{9}{4G} \Delta^{\nu*}_\mu \Delta^\nu_\mu - \frac{1}{\Omega} \sum_{p,n}{}' (v_F(p-k_F) - E_{p,n}) + \frac{2T}{\Omega} \sum_{p,n}{}' \ln\left(1 + \exp\left(-\frac{E_{p,n}}{T}\right)\right) \tag{2.28}$$

In the massless limit, $\lambda = 0$, the off-diagonal elements of the 2×2 matrix in (2.26) vanish and we are left with only the transverse pairing.

3. THE THERMODYNAMICS OF THE SPIN-1 COLOR SUPERCONDUCTIVITY

The polar, A, planar and CSL are the four canonical phases mostly discussed in the literature of the spin-1 color superconductivity. Each of them corresponds to a particular diagonal form of the 3×3 matrix Δ_a^c introduced in the last section. The thermodynamics will be discussed in this section for an arbitrary quark mass.

To gain more insight to the geometrical structure of these spin-1 phases, we introduce the following two sets of spherical basis

$$\mathbf{e}_\pm \equiv \mp\frac{1}{\sqrt{2}}(\hat{\mathbf{x}}\pm i\hat{\mathbf{y}}) \qquad \mathbf{e}_0\equiv\hat{\mathbf{z}} \tag{3.1}$$

and

$$\epsilon_\pm \equiv \mp\frac{e^{\pm i\varphi}}{\sqrt{2}}(\hat{\theta}\pm i\hat{\varphi}) \qquad \epsilon_0\equiv\hat{\mathbf{p}} \tag{3.2}$$

where $\hat{\theta}$, $\hat{\varphi}$ and $\hat{\mathbf{p}}$ are the unit vectors in the directions of increasing θ, φ and p of the spherical coordinates of momentum $\mathbf{p}$, given by

$$\begin{aligned}\hat{p} &= (\sin\theta\cos\varphi,\sin\theta\sin\varphi,\cos\theta)\\ \hat{\theta} &= (\cos\theta\cos\varphi,\cos\theta\sin\varphi,-\sin\theta)\\ \hat{\varphi} &= (-\sin\varphi,\cos\varphi,0)\end{aligned} \tag{3.3}$$

The extra phase factor $e^{\pm i\varphi}$ renders $\epsilon_\pm$ nonsingular at the north pole, $\theta=0$. It is straightforward to verify that

$$D^1_{\alpha\beta}(\varphi,\theta,-\varphi)=\mathbf{e}^*_\alpha\cdot\epsilon_\beta \tag{3.4}$$

and the gap matrix takes the compact form

$$M=\sqrt{3}\Delta^\beta_\alpha\begin{pmatrix}(\epsilon_+)_\alpha{}^* & \frac{\lambda}{\sqrt{2}}(\epsilon_0)_\alpha{}^*\\ \frac{\lambda}{\sqrt{2}}(\epsilon_0)_\alpha{}^* & (\epsilon_-)^*_\alpha\end{pmatrix}J_\beta \tag{3.5}$$

where the indexes α and β run over either the spherical basis (3.1) or cartesian basis $\hat{\mathbf{x}}$, $\hat{\mathbf{y}}$ and $\hat{\mathbf{z}}$.

Now we are ready to introduce the four canonical spin-1 phases in terms of the circular basis (3.1), with respect to which

$$\vec{J}=-\frac{1}{\sqrt{2}}J_-\mathbf{e}_+ +\frac{1}{\sqrt{2}}J_+\mathbf{e}_- +J_0\mathbf{e}_0 \tag{3.6}$$

with $J_\pm=J_x\pm iJ_y$ and $J_0=J_z$. Each of the canonical phases corresponds to a particular form of the 3×3 matrix Δ^β_α in (3.5)(with α labelling the rows and β the columns). We have

$$\Delta(\text{polar})=\Delta\text{diag.}(0,0,1) \tag{3.7a}$$

$$\Delta(\text{A})=\Delta\begin{pmatrix}0&0&1\\0&0&0\\0&0&0\end{pmatrix}\ \text{or}\ \Delta(\text{A})=\Delta\begin{pmatrix}0&0&0\\0&0&1\\0&0&0\end{pmatrix} \tag{3.7b}$$

$$\Delta(\text{planar})=\frac{1}{\sqrt{2}}\Delta\text{diag.}(1,1,0) \tag{3.7c}$$

$$\Delta(\text{CSL})=\frac{1}{\sqrt{3}}\Delta\text{diag.}(1,1,1) \tag{3.7d}$$

where Δ is the gap parameter to be determined.

Correspondingly, the gap matrix

$$M(\text{polar})=\sqrt{\frac{3}{2}}\Delta\begin{pmatrix}J_0e^{-i\varphi}\sin\theta & J_0\lambda\cos\theta\\ J_0\lambda\cos\theta & -J_0e^{i\varphi}\sin\theta\end{pmatrix} \tag{3.8}$$

$$M(\mathrm{A}) = \sqrt{3}\Delta \begin{pmatrix} -J_0 \cos^2\frac{\theta}{2} & \frac{\lambda}{2} J_0 e^{i\varphi}\sin\theta \\ \frac{\lambda}{2} J_0 e^{i\varphi}\sin\theta & -J_0 e^{2i\varphi}\sin^2\frac{\theta}{2} \end{pmatrix} \tag{3.9}$$

$$M(\mathrm{planar}) = \frac{\sqrt{3}}{2}\Delta \begin{pmatrix} -J_- \cos^2\frac{\theta}{2} + J_+ e^{-2i\varphi}\sin^2\frac{\theta}{2} & \frac{\lambda}{2}(J_- e^{i\varphi} + J_+ e^{-i\varphi})\sin\theta \\ \frac{\lambda}{2}(J_- e^{i\varphi} + J_+ e^{-i\varphi})\sin\theta & -J_- e^{2i\varphi}\sin^2\frac{\theta}{2} + J_+\cos^2\frac{\theta}{2} \end{pmatrix} \tag{3.10}$$

and

$$M_{\mathrm{CSL}} = \sqrt{\frac{1}{2}}\Delta \begin{pmatrix} -e^{-i\varphi}\mathcal{J}_- & \lambda\mathcal{J}_0 \\ \lambda\mathcal{J}_0 & e^{i\varphi}\mathcal{J}_+ \end{pmatrix} \tag{3.11}$$

The operators $\mathcal{J}_\pm$ and $\mathcal{J}_0$ inside M_{CSL} are defined by

$$\mathcal{J}_\pm = \epsilon^*_\mp \cdot \mathbf{J} = \pm e^{\pm i\varphi}(J_\theta \pm i J_\varphi) \qquad \mathcal{J}_0 = \epsilon^*_0 \cdot \mathbf{J} \tag{3.12}$$

with $J_\theta = \hat{\theta}\cdot\mathbf{J}$ and $J_\varphi = \hat{\varphi}\cdot\mathbf{J}$. They satisfy the same angular momentum algebra as $J_\pm$ and J_0 in (3.6).

Though the gap matrices (3.8), (3.9), (3.10) and (3.11) looks complicated, analytical expressions of the eigenvalues of $MM^\dagger$ or $M^\dagger M$ can be obtained for an arbitrary quark mass. Parametrizing the eigenvalues by $\Delta^2 f^2(\theta)$, we find that

$$f^2(\theta) = \begin{cases} (1/8)\left(\sqrt{\lambda^2+8}\pm\lambda\right)^2 (d_i=2),\ \frac{1}{2}\lambda^2(d_i=2) & \text{for CSL phase} \\ (3/4)\left(\cos^2\theta + 1 + \lambda^2\sin^2\theta\right)(d_i=4),\ 0(d_i=2) & \text{for planar phase} \\ (3/2)\left(\sin^2\theta + \lambda^2\cos^2\theta\right)(d_i=4),\ 0(d_i=2) & \text{for polar phase} \\ (3/4)\left(1\pm\sqrt{\lambda^2\sin^2\theta+\cos^2\theta}\right)^2 (d_i=2),\ 0(d_i=2) & \text{for A phase} \end{cases} \tag{3.13}$$

where the integer inside the parentheses following each expression indicates the degeneracy of each distinct eigenvalue. The details of the diagonalization is shown in Appendix B. The function $f(\theta)$ is θ-dependent for the polar, A and planar phases and we shall refer to these phases as nonspherical. The CSL phase will be referred to as spherical because of the constancy of its $f(\theta)$.

Then the pressure corresponding to (2.28) becomes:

$$P = -\frac{9}{4G}\Delta^2 - \frac{1}{\Omega}\sum_{p,i}\frac{d_i}{2}(v_F(p-k_F) - E_{p,i}) + \frac{T}{\Omega}\sum_{p,i} d_i \ln\left(1+\exp\left(-\frac{E_{p,i}}{T}\right)\right) \tag{3.14}$$

where $E_{p,i} = \sqrt{v_F^2(p-k_F)^2 + \Delta^2 f_i^2(\theta)}$. Here the index i labels the distinct eigenvalues in each line of (3.13) with d_i the degeneracy. The summation over the entire momentum space is restored owing to the symmetry of $f(\theta)$'s under space inversion. Maximizing the pressure with respect to Δ, we obtain the gap equation $\left(\frac{\partial P}{\partial \Delta^2}\right)_{T,\mu} = 0$, which determines the temperature dependence of the gap, $\Delta(T)$, up to the transition temperature.

In terms of the parameter $t = \frac{\Delta(T)}{T}$, the gap equation takes the form $\ln\frac{\Delta(0)}{\Delta(T)} = \frac{h(t)}{2+\lambda^2}$ with

$$h(t) = \sum_i \frac{d_i}{2}\int_0^\pi d\theta \sin\theta f_i^2(\theta)\int_0^\infty dx \frac{1}{\sqrt{x^2+t^2 f_i^2(\theta)}[e^{\sqrt{x^2+t^2 f_i^2(\theta)}}+1]} \tag{3.15}$$

It follows that

$$T = \frac{\Delta(0)}{t} e^{-\frac{h(t)}{2+\lambda^2}} \tag{3.16}$$

The condensation energy density of the CSC is given by

$$P_s - P_n \equiv \rho_s(t)\frac{\mu^2\Delta_0^2}{2\pi^2} \tag{3.17}$$

with s labeling different pairing states and $\Delta_0 \equiv \Delta_{\mathrm{CSL}}(0)$ when $m_s = 0$ and we have

$$\rho_s(t) = v_F e^{-\frac{2}{2+\lambda^2}h(t)}\left[\frac{2+\lambda^2}{2} + h(t) + 2\frac{g(t)}{t^2} - a\frac{\pi^2}{t^2}\right] \tag{3.18}$$

with $a = \frac{2}{3}(1)$ for nonspherical(spherical) phase and

$$g(t) = \sum_i \frac{d_i}{2} \int_0^\pi d\theta \sin\theta \int_0^\infty dx \ln[e^{-\sqrt{x^2+t^2 f_i^2(\theta)}} + 1] \tag{3.19}$$

The curves $P(T)$ may be plotted parametrically according to (3.16) and (3.18) without solving the gap equation for $T > 0$, as we did in [14]. The transition temperature T_c^λ is determined by (3.16) in the limit $t \to 0$ with $\Delta(0)$ the solution of the gap equation at $T = 0$. We find that

$$T_c^\lambda = (\frac{2K}{\Delta_0})^{(1-\frac{2}{2+\lambda^2}\frac{1}{v_F})} T_c^0 \tag{3.20}$$

where K is a UV cutoff for $\mid p - k_F \mid$ in the momentum integration and is assumed to satisfy the condition $\Delta_0 << K << k_F$. We set $K = 27$MeV for the numerical calculation in this paper. For a given mass, T_c^λ is universal to all four phases and the ratio between the pressures of different phases is independent of the cutoff K. This cutoff matters only when we compare the gaps and pressures of different mass values. With Fermi velocity $v_F = \sqrt{1-\lambda^2}$, T_c^λ is a monotonic decreasing function of λ for $0 \le \lambda < 1$. Then the transition temperature with massive quarks is always lower than that in the massless limit. The factor ρ_s vanishes at the transition temperature T_c^λ. When $\lambda = 0$, the corresponding curves of $\rho_s(T)$ is the same with what we got in [14] in the ultra-relativistic limit. We have $\rho_{\rm CSL} = 1$, $\rho_{\rm planar} = 0.98$, $\rho_{\rm polar} = 0.88$ and $\rho_{\rm A} = 0.65$ at $T = 0$, in agreement with the values reported in [12]. In the non-relativistic limit, we get $\rho_{\rm polar} = \rho_{\rm planar} = 2\rho_{\rm A} = \frac{2^{4/3}}{3}\rho_{\rm CSL}$, consistent with the results in [10].

The factor ρ_s versus T/T_c^λ is plotted in Fig.1 for $\lambda = 0.3$ and $\lambda = 0.6$. For $\mu = 500$MeV, the former corresponds to $m = 150$MeV and the latter to $m = 300$MeV. The curves of Fig.1 implies the same inequality

$$P_n < P_{\rm A} < P_{\rm polar} < P_{\rm planar} < P_{\rm CSL} \tag{3.21}$$

as in the massless limit($\lambda = 0$). We expect (3.21) to hold within the whole domain of $0 \le \lambda < 1$.

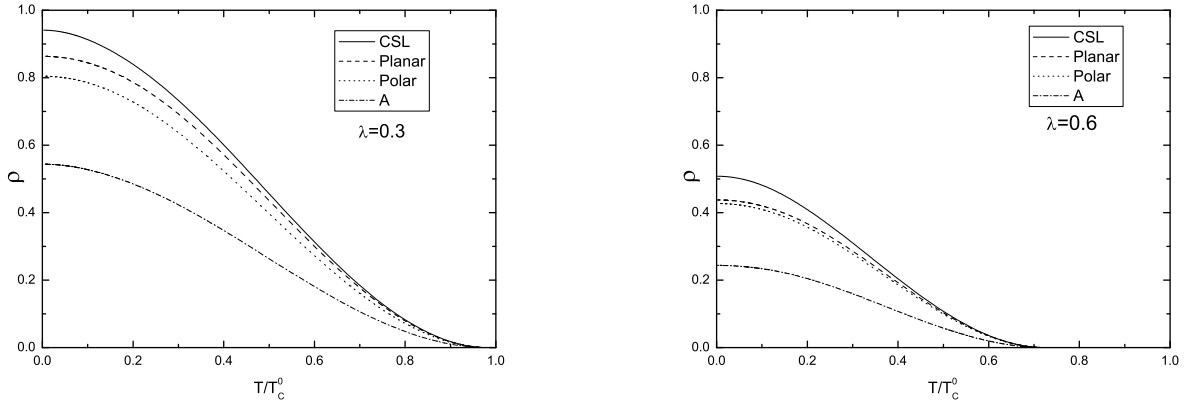

FIG. 1: The scaled condensation energy dependence on temperature with different masses $\lambda = 0.3$ and $\lambda = 0.6$.

In what follows, we shall identify $\Delta_{\rm CSL}(0)$ with that of the one-gluon exchange [10, 17],

$$\Delta_0 = 512\pi^4 \left(\frac{2}{3}\right)^{\frac{5}{2}} \frac{\mu}{g^5} \exp\left(-\frac{3\pi^2}{\sqrt{2}g} - \frac{\pi^2+4}{8} - 9\right) \tag{3.22}$$

extrapolated to $\mu = 500MeV$ and $\alpha_s = \frac{g^2}{4\pi} = 1$ with g the QCD running coupling constant. We can obtain the transition temperature $T_c^{\lambda=0} = \frac{e^{\gamma_E}}{\pi}\Delta_0$ for u and d quarks in MeV. The transition temperature of s quarks, of $T_c^{\lambda\neq 0}$ follows from (3.20). For $K = 27$MeV, we find $T_c^{0.3} = 0.98T_c^0$ for $m_s = 150$MeV and $T_c^{0.6} = 0.683T_c^0$ for $m_s = 300$MeV. We should notice that the screening effect underlying the formulas (3.22) comes from all three flavors in the massless limit. This inconsistency, however, will not affect our order of magnitude estimation.

4. THE PHASE DIAGRAM IN A MAGNETIC FIELD

The physics of a quark matter in a magnetic field has received increasing attention because of the presence of a strong magnetic field in a compact star or during a noncentral collision of heavy-ions. The phase structure of 2SC in a magnetic field has been investigated in [18, 19]. Equation of state for the CFL phase in a magnetic field and its implications for compact star models have been studied in [20]. For an ultra-strong magnetic field B, the spacing of Landau levels becomes comparable or larger than the quark chemical potential, i.e. $\sqrt{eB} \geq \mu$, the magnetic field will impact on the pairing dynamics of CFL [21]. For the typical value of μ(=500MeV), this requires that $B > 10^{18}$G, which may be implemented inside some magnetar. It was shown in [21] that an ultra-strong magnetic field may enhance the energy gap of the CFL for $\sqrt{eB} >> \mu$ and induce a magnetic moment of a Cooper pair. At a weaker magnetic field, $\sqrt{eB} >> \mu$, a de-Hass van-Alphen oscillation of the energy gap has been found [23, 24]. Alternatively a domain structure may be formed because of the chiral symmetry breaking and the axial anomaly [18]. For a spin-1 CSC, in additional to above possibilities, a magnetic field may offset the balance between the CSL and nonspherical phases, producing a rich phase structure with respect to the temperature and the field shown in our previous work [14]. This mechanism will be further explored below taking into account the nonzero mass of strange quarks.

The discussions of proceeding sections imply a nonzero order parameter

$$\Phi =< \bar{\psi}_C \Gamma^c \lambda^c \psi > \tag{4.1}$$

in the coordinate space, where ψ is the quark field, $\psi_C = \gamma_2 \psi^*$ is its charge conjugate, λ^c with $c = 2, 5, 7$ is an antisymmetric Gell-Mann matrices and Γ^c is a 4×4 spinor matrix. We may choose $\Gamma^5 = \Gamma^7 = 0$ for the polar and A phases, $\Gamma^2 = 0$ for the planar phase but none of Γ^c's vanishes for CSL phase. Depending on the symmetry of (4.1), their responses to an external magnetic field are quite different.

For CSL phase, the diquark condensate (4.1) breaks the gauge symmetry $\mathrm{SU}(3)_c \times \mathrm{U}(1)_{\mathrm{em}}$ completely. But the Meissner effect for a nonspherical condensate is incomplete, because it breaks the gauge symmetry partially. Among the residual gauge group, which leaves the diquark operator inside (4.1) unchanged, there exists a U(1) transformation, $\psi \to e^{-\frac{i}{2}\lambda_8 \theta - iq\phi}\psi$ with q the electric charge of ψ, $\theta = -2\sqrt{3}q\phi$ for the polar and A phases and $\theta = 4\sqrt{3}q\phi$ for the planar phase. The corresponding gauge field, $\mathcal{A}_\mu$ is identified with the electromagnetic field in the condensate and is related to the electromagnetic field A and the 8-th component of the color field A^8 in the normal phase through a U(1) rotation

$$\begin{aligned} \mathcal{A}_\mu &= A_\mu \cos\gamma - A^8_\mu \sin\gamma \\ \mathcal{V}_\mu &= A_\mu \sin\gamma + A^8_\mu \cos\gamma \end{aligned} \tag{4.2}$$

where the mixing angle γ is given by $\tan\gamma_{\mathrm{polar,A}} = 2\sqrt{3}q(e/g)$ and $\tan\gamma_{\mathrm{planar}} = 4\sqrt{3}q(e/g)$ for planar. The 2nd component of (4.2) $\mathcal{V} = 0$ because of the Meissner effect and thereby imposes a constraint inside a nonspherical CSC, $A^8_\mu = -A_\mu \tan\gamma$, which implies that:

$$\mathbf{B}^8 = -\mathbf{B}\tan\gamma \tag{4.3}$$

with $\mathbf{B} = \nabla \times \mathbf{A}$.

Expressing the gauge coupling $\bar{\psi}\gamma_\mu(eqA_\mu + A^8_\mu \lambda_8/2)\psi$ in terms of $\mathcal{A}_\mu$ and its orthogonal partner $\mathcal{V}_\mu$, we extract the electric charges with respect to $\mathcal{A}$ in color space,

$$Q = \begin{cases} \dfrac{3qg}{\sqrt{g^2 + 12q^2e^2}}\mathrm{diag.}(0,0,1) & \text{for polar and A} \\ \dfrac{3qg}{\sqrt{g^2 + 48q^2e^2}}\mathrm{diag.}(1,1,-1) & \text{for planar} \end{cases} \tag{4.4}$$

Because of the nonzero charges of pairing quarks, the planar state is subject to the impact of Landau orbitals in a magnetic field, like that for CFL.

The thermal equilibrium in a magnetic field $H\hat{\mathbf{z}}$ is determined by minimizing the Gibbs free energy density,

$$\mathcal{G} = -P + \frac{1}{2}B^2 + \frac{1}{2}\sum_{l=1}^{8}(B^l)^2 - BH \tag{4.5}$$

with respect to Δ, B and B^l. Ignoring the induced magnetization of quarks, the pressure P is given by (2.4), with Δ given by the solution of the gap equation. Ignoring the induced magnetization of quarks, the pressure P is given

TABLE I:

	I	II	III	IV
2 flavor	$\mathrm{CSL_u}, \mathrm{CSL_d}$	$(\mathrm{polar})_\mathrm{u}, (\mathrm{planar})_\mathrm{d}$	$(\mathrm{normal})_\mathrm{u}, (\mathrm{polar})_\mathrm{d}$	$(\mathrm{normal})_\mathrm{u}, (\mathrm{normal})_\mathrm{d}$
3 flavor	$\mathrm{CSL_u}, \mathrm{CSL_{d,s}}$	$(\mathrm{polar})_\mathrm{u}, (\mathrm{planar})_\mathrm{d,s}$	$(\mathrm{normal})_\mathrm{u}, (\mathrm{polar})_\mathrm{d,s}$	$(\mathrm{normal})_\mathrm{u}, (\mathrm{normal})_\mathrm{d,s}$

by (2.4), with Δ given by the solution of the gap equation. For a nonspherical CSC pairing, the minimization with respect to B and B^l is subject to the constraint (4.3). For a hypothetical quark matter of one flavor only, we find that

$$\mathcal{G}_{\mathrm{min.},j} = -P_j - \frac{1}{2}\eta_j H^2 \tag{4.6}$$

with $j = n$, CSL, polar, A and planar, where $\eta_n = 1$, $\eta_{\mathrm{CSL}} = 0$ and $\eta_j = \cos^2\gamma_j$ for a nonspherical CSC. The phase corresponding to minimum among $\mathcal{G}_{\mathrm{min}}$'s above wins the competition and transition from one phase to another is first order below T_c.

The situation becomes more subtle when quarks of different flavors coexist even though pairing is within each flavor. Different electric charges of different quark flavors imply different mixing angles which may not be compactible with each other. Consider, for instance, a quark matter of u and d flavors with each flavor in a non-spherical CSC state with different mixing angles. (4.3) imposes two constraints, which are consistent with each other only if $B = B^8 = 0$. Then we end up with an effective Meissner shielding [11], making it fail to compete with the phase with both flavors in CSL states. On the other hand, one may relax the constraints by assuming that the basis underlying the condensate of u quarks differ from that underlying the condensate of d quarks by a color rotation. Consequently the constraint (4.3) for each flavor reads $B^8 = -B\tan\gamma^u$ and $B'^8 = -B\tan\gamma^d$. If both flavors stay in the polar or A phases, which allows $\mathbf{B}^{1-3}$ to penetrate in, one may expect that an orthogonal transformation

$$\begin{aligned} B'^8 &= B^8\cos\beta - B^3\sin\beta \\ B'^3 &= B^8\sin\beta + B^3\cos\beta \end{aligned} \tag{4.7}$$

could compromise both constraints. Such a transformation, however, lies outside the color $SU(3)$ group and therefore, the mutual rotation of color basis is not an option. The phases of the two flavor quark matter (u, d) without Meissner effects, which can compete with (CSL, CSL), include (polar, planar), (polar(normal), normal(polar)), (A(normal), normal(A)) and (normal, normal). Notice the coincidence of the mixing angle of the polar state of u quarks and that of the planar state of d quarks. Also the normal phase does not impose any constraint on the gauge field and can coexist with any nonspherical CSC.

The Gibbs free energies remain given by the equations of (4.6), but with P_n and P_{CSL} referring to the total pressure of all quarks for normal and CSL phases. For nonspherical phases, P is the total pressure of all flavors with at least one of them in a nonspherical CSC state and γ is their common mixing angle. For normal-CSC combination, γ refers to that of the CSC state. The number of combinations to be examined is reduced by two criteria: 1) For two combinations of the same mixing angle, the one with higher pressure wins. 2) For two combinations of the same pressure, the one with smaller magnitude of the mixing angle wins. Because the function ρ_s for various CSC phases also satisfy the inequalities (3.21) up to the transition temperature for an arbitrary mass, it follows that there are only four phases to be considered in each case of two and three flavors with nonzero quark masses, which are shown in Table I.

The border between two phases are determined by the equation

$$P_\alpha + \eta_\alpha\frac{H^2}{2} = P_\beta + \eta_\beta\frac{H^2}{2} \tag{4.8}$$

with the subscripts α and β labelling the four phases I-IV.

In a multiflavor quark matter the Fermi momentum of each flavor is displayed from each other to meet the charge neutrality requirement (The color neutrality condition is ignored owing to the small energy gap associated to the single flavor pairing). In what follows, we shall consider the quark matter of two massless flavors ($m_u = m_d = 0$) and a massive flavor ($m_s \neq 0$), coexists with electrons. Within the mean-field approximation employed in proceeding sections, the Fermi-momentum displacement can be determined in the ideal gas limit at zero temperature. The total pressure under this approximation reads

$$P^{(0)} = -\sum_f E_f - E_e + \mu\sum_f n_f + \mu_q\left(\sum_f q_f n_f - n_e\right) \tag{4.9}$$

where E_f, n_f and n_f^q are the kinetic energy density and number density of the quark flavor f with $f = u, d, s$ and $q_f = (2/3, -1/3, -1/3)$, E_e and n_e are corresponding quantities for electrons. A charge chemical potential μ_q is introduced with the (...) of (4.9) the charge number density. We have

$$E_f = \frac{3}{\pi^2}\int_0^{k_f} dpp^2\sqrt{p^2+m_f^2} \qquad E_e = \frac{k_e^4}{4\pi^2} \tag{4.10}$$

$$n_f = \frac{1}{\pi^2}k_f^3 \qquad n_e = \frac{1}{3\pi^2}k_e^3 \tag{4.11}$$

with $m_f = (0, 0, m_s)$. The Fermi momenta, k_f and k_e are determined by the equilibrium conditions

$$\left(\frac{\partial P^{(0)}}{\partial k_f}\right)_{\mu,\mu_q} = \left(\frac{\partial P^{(0)}}{\partial k_e}\right)_{\mu,\mu_q} = 0 \tag{4.12}$$

and the charge neutrality constraint

$$\sum_f q_f n_f - n_e = 0 \tag{4.13}$$

We find that $k_u = 1.001\mu$, $k_d = 1.01$ and $k_s = 0.941\mu$ for $m_s = 0.3\mu$, and that $k_u = 1.004\mu$, $k_d = 1.039\mu$ and $k_s = 0.744\mu$ for $m_s = 0.6\mu$. We got this H-T diagram, Fig.2, and H_0 is defined by

$$H_0 = \frac{\mu\Delta_0}{\pi} \tag{4.14}$$

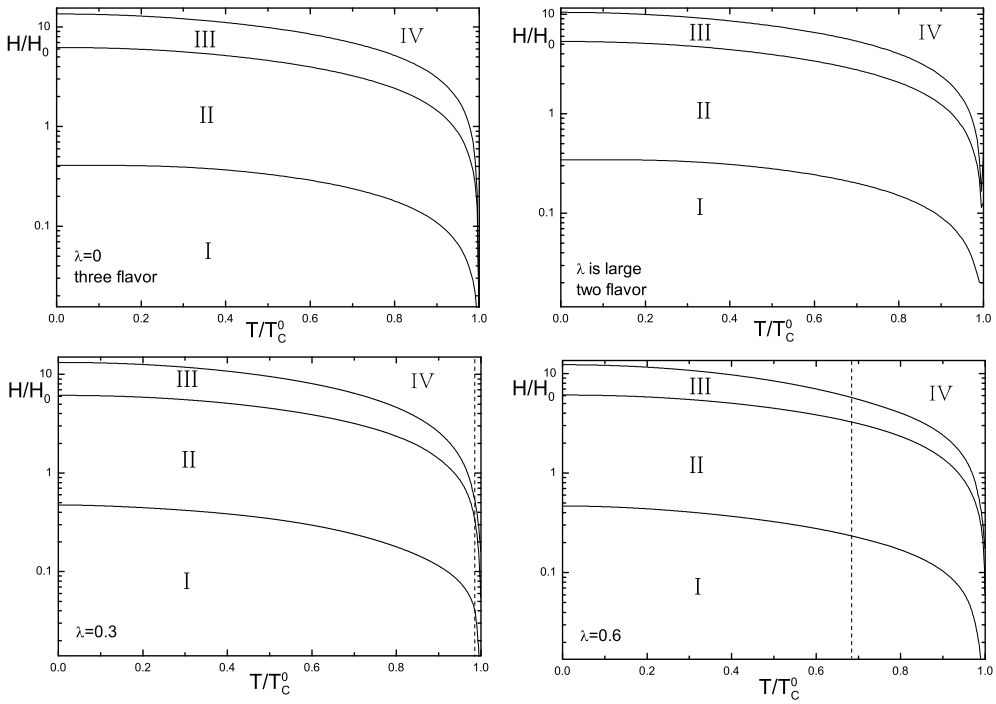

FIG. 2: H-T phase diagram. These four diagrams corresponding to the ultra-relativistic limit $m_s = 0$, $m_s >> \mu$ and $m_s = 150MeV$, $m_s = 300MeV$.

When the strange quark mass is ignored, the transition temperature of all flavors are the same, this three flavor phase is what we got in the diagram "$\lambda = 0$". The transition from one to another is first order. When we assume a large mass of s quarks, $m_s >> \mu$, This two flavor case is certainly unrealistic. When m_s is comparable to μ, the transition temperature of strange quark parings is reduced, so when $T_c^\lambda < T < T_c^0$, strange quarks become unpaired, while u and d quark parings remain. Below T_c^λ, the condensation energy of strange quarks rises like $(T_c^\lambda - T)^2$. The transition from three flavor CSC to two flavor CSC is therefore of second order at zero magnetic field. Since only the condensation energy, not its derivatives, enters (4.8), both the phase boundaries and their slopes with respect to the temperature are continuous at T_c^λ. The dashed line in Fig.2 is the border between the three flavor region and the two flavor region in the phase diagram. In the left region of the dashed line, the corresponding phases combination is "3 flavor" in the Table.I, and the right region is corresponding to the upper line "2 flavor". The values of the bounder between two regions is close to these in massless limit in three flavor, also these nonspherical phases occupy a significant portion of the H-T phase diagram for a magnitude of the magnetic field of order $10^{14}G$. This strong magnetic field is plausible in a compact star. Due to the not apparent change to the border between the possible phases, the physical implications of the mass effect to the cooling behaviors or the latent heat released as the star cools through the phase boundaries won't be discussed in this paper, it won't give corrections in order with [22]. The smallness of the spin-1 gap makes CSC being of type I and the critical magnetic field $B \sim \mu\Delta_0 << \mu^2/e$. Therefore, the magnetic impact on the pairing dynamics as well as the quark matter magnetization may be neglected [22], unlike the situation considered in [21, 23, 24].

5. CONCLUDING REMARKS

For the quark matter of moderate density, such as that may reside in the core of a compact star, the mass of strange quarks, m_s, is not much smaller than the quark chemical potential μ and need to be taken into account. In this paper, we extend the study of the four single flavor phases of color superconductivity to include the effect of the nonzero m_s. In spite of the complication of the coupling between the cross-helicity and equal helicity channels, the excitation spectrum is obtained analytically. We have explored its correction to the pressure and the transition temperature numerically. It is found that mass effect reduces the pressure and transition temperature of strange quarks, but it doesn't change the ranking $P_n < P_{\rm A} < P_{\rm polar} < P_{\rm planar} < P_{\rm CSL}$ of the pressure for the four canonical single flavor phases for the values of m_s we examined. We suspect that the above inequality holds for an arbitrary m_s. Then we generalized the previous work to the quark matter with massless u and d flavors and the massive s flavor. Because the transition temperature for strange quark parings is lower than that of massless quark pairings, this new H-T diagram consists of the two flavor CSC for $T_c^\lambda < T < T_c^0$ and the three flavor CSC for $0 < T < T_c^\lambda$. The three flavor and the two flavor region will be occupied by the same phases I-IV in Table I with the same relative positions. There is a second order phase transition from three flavor condensate to two flavor condensate at transition temperature T_c^λ where strange quarks condense. The phase boundaries in the two regions join smoothly. As an order of magnitude estimate, we calibrated our model T_c against the that from the QCD one-gluon exchange in the chiral limit and found the typical magnitude of the magnetic field in the phase diagram falls within the range of the plausible magnetic field inside a compact star in the literature.

On the other hand, the effective Lagrangian (2.1) we employed in this paper is by no means the most general one. The Lorentz covariance of (2.1) is unlikely in a medium and the coupling G may depends on m_s. Taking the one-gluon exchange as a reference, the screenings of the color magnetic channel and the color electric one by the medium are very different and should depends the masses of quarks. These properties is likely to persists qualitatively at the moderate density and should be reflected in the effective action to some extents. Also, the inequality (3.21) may not be as robust as people thought. A purely Ginzburg-Landau analysis [25] reveals some parameter region where the ranking (3.21) is offset even without a magnetic field. The microscopic mechanism supporting this observation, based on the most general four-fermion effective action or others, remains to be unveiled.

Throughout this paper, we take the massless limit of u and d flavors and then gapless excitations exist in all I-IV phases of Table.I. In reality, the chiral restoration transition from low density to high density may be a crossover and u and d quarks may also acquire nonzero masses from the chiral condensate. Consequently, the excitations of the phase I where all flavors are in CSL will be gapped. This is welcome since it will slow down the direct Urca processes of cooling in a compact star by spin-1 CSC alone [16]. But the gapless modes remains for nonspherical states and phase diagrams Fig.2 are still valid qualitatively. Therefore the magnetic field inside the star cannot exceed the magnitude along the border line between I and II of Fig.2 for a slow cooling process.

Acknowledgments

The authors are grateful to Thomas Schäfer for a communication on the NR limit. We would like to extend our gratitude to Bo Feng for useful discussions. The work of D. F. H. and H. C. R. is supported in part by NSFC under grant Nos. 10575043, 10735040,11135011.

Appendix A

In this appendix, we shall fill in the details from (2.11) to (2.18). Substituting (2.13) and (2.17) into (2.12), we obtain that

$$\begin{aligned} A_{s_1',s_2';s_1,s_2}(\mathbf{p}',\mathbf{p}) &= 2C_{s_1's_2'}(\mathbf{p}')C_{-s_2-s_1}(\mathbf{p})\phi^\dagger_{\mathbf{p}',s_1'}\bar\sigma^\nu\phi_{-\mathbf{p},s_2}\phi^\dagger_{-\mathbf{p}',s_2'}\bar\sigma^\nu\phi_{\mathbf{p},s_1} \\ &+ 2C_{-s_1'-s_2'}(\mathbf{p}')C_{s_2s_1}(\mathbf{p})\phi^\dagger_{\mathbf{p}',s_1'}\sigma^\nu\phi_{-\mathbf{p},s_2}\phi^\dagger_{-\mathbf{p}',s_2'}\sigma^\nu\phi_{\mathbf{p},s_1} \\ &+ 2C_{s_1'-s_2'}(\mathbf{p}')C_{-s_2s_1}(\mathbf{p})\phi^\dagger_{\mathbf{p}',s_1'}\bar\sigma^\nu\phi_{-\mathbf{p},s_2}\phi^\dagger_{-\mathbf{p}',s_2'}\sigma^\nu\phi_{\mathbf{p},s_1} \\ &+ 2C_{-s_1's_2'}(\mathbf{p}')C_{s_2-s_1}(\mathbf{p})\phi^\dagger_{\mathbf{p}',s_1'}\sigma^\nu\phi_{-\mathbf{p},s_2}\phi^\dagger_{-\mathbf{p}',s_2'}\bar\sigma^\nu\phi_{\mathbf{p},s_1} \end{aligned} \tag{A.1}$$

where $C_{ss'}(p)=\frac{\sqrt{(E+2sp)(E+2s'p)}}{2E}$ It follows from the identity

$$(\sigma_j)_{\alpha\beta}(\sigma_j)_{\gamma\delta}=2\delta_{\alpha\delta}\delta_{\beta\gamma}-\delta_{\alpha\beta}\delta_{\gamma\delta} \tag{A.2}$$

that

$$\begin{aligned} \phi^\dagger_{\mathbf{p}',s_1'}\bar\sigma^\nu\phi_{-\mathbf{p},s_2}\phi^\dagger_{-\mathbf{p}',s_2'}\bar\sigma^\nu\phi_{\mathbf{p},s_1} &= \phi^\dagger_{\mathbf{p}',s_1'}\sigma^\nu\phi_{\mathbf{p},s_2}\phi^\dagger_{-\mathbf{p}',s_2'}\sigma^\nu\phi_{-\mathbf{p},s_1} \\ &= 2\phi^\dagger_{\mathbf{p}',s_1'}\phi_{-\mathbf{p},s_2}\phi^\dagger_{-\mathbf{p}',s_2'}\phi_{\mathbf{p},s_1}-2\phi^\dagger_{\mathbf{p}',s_1'}\phi_{\mathbf{p},s_1}\phi^\dagger_{-\mathbf{p}',s_2'}\phi_{-\mathbf{p},s_2} \\ \phi^\dagger_{\mathbf{p}',s_1'}\bar\sigma^\nu\phi_{-\mathbf{p},s_2}\phi^\dagger_{-\mathbf{p}',s_2'}\sigma^\nu\phi_{\mathbf{p},s_1} &= \phi^\dagger_{\mathbf{p}',s_1'}\sigma^\nu\phi_{-\mathbf{p},s_2}\phi^\dagger_{-\mathbf{p}',s_2'}\bar\sigma^\nu\phi_{\mathbf{p},s_1} \\ &= 2\phi^\dagger_{\mathbf{p}',s_1'}\phi_{\mathbf{p},s_1}\phi^\dagger_{-\mathbf{p}',s_2'}\phi_{-\mathbf{p},s_2} \end{aligned} \tag{A.3}$$

For two different momenta, $\mathbf{p}$ and $\mathbf{p}'$, we have

$$\phi^\dagger_{\mathbf{p}',s'}\phi_{\mathbf{p},s}=(D^{\frac12\dagger}(\varphi',\theta',-\varphi')D^{\frac12}(\varphi,\theta,-\varphi))_{s's}=D^{\frac12}_{s's}(R) \tag{A.4}$$

where R stands for the Euler angles corresponding to the product of the rotations specified by $(\varphi,\theta,-\varphi)$ and $(\varphi',\theta',-\varphi')$. Together with the orthonormal relation $\phi^\dagger_{\mathbf{p},s}\phi_{\mathbf{p},s'}=\delta_{ss'}$, we obtain that

$$\begin{aligned} &A_{s_1',s_2';s_1,s_2}(\mathbf{p}',\mathbf{p}) \\ =\ & 4(-1)^{s_2+s_2'-1}e^{i(-\theta_{\mathbf{p}s_2}+\theta_{\mathbf{p}'s_2'})}C_{s_1's_2'}(p')C_{-s_2-s_1}(p)e^{i(-\theta_{\mathbf{p}-s_2}+\theta_{\mathbf{p}'-s_2'})}(D^{\frac12}_{s_1'-s_2}(R)D^{\frac12}_{-s_2's_1}(R)-D^{\frac12}_{s_1's_1}(R)D^{\frac12}_{-s_2'-s_2}(R)) \\ +\ & 4(-1)^{s_2+s_2'-1}C_{s_1'-s_2'}(p')C_{s_1-s_2}(p)e^{i(-\theta_{\mathbf{p}s_2}+\theta_{\mathbf{p}'s_2'})}D^{\frac12}_{s_1'-s_2}(R)D^{\frac12}_{-s_2's_1}(R) \end{aligned} \tag{A.5}$$

where the phase $\theta_{\mathbf{p},\mathbf{s}}$ is defined in (2.20) and satisfies the relation

$$e^{i\theta_{-\mathbf{p},s}}=-e^{i\theta_{\mathbf{p},s}} \tag{A.6}$$

Because

$$D^{\frac12}_{s_1'-s_2}(R)D^{\frac12}_{-s_2's_1}(R)-D^{\frac12}_{s_1's_1}(R)D^{\frac12}_{-s_2'-s_2}(R))=detD^{\frac12}(R)\epsilon_{s_1'-s_2'}\epsilon_{s_1-s_2}=\epsilon_{s_1'-s_2'}\epsilon_{s_1-s_2} \tag{A.7}$$

in (A.5), $\epsilon_{s_1'-s_2'}\epsilon_{s_1-s_2}\neq0$ requires that $s_1'=s_2', s_1=s_2$. Then the diquark operator of equal helicity is even in $\mathbf{p}$ because of the equation (2.20), so sum over $\mathbf{p}$ will make it vanish on account of (A.6). So this part doesn't contribute.

Using the formula of Wigner D-functions

$$D^A_{aa'}(\alpha,\beta,\gamma)D^B_{bb'}(\alpha,\beta,\gamma)=\sum_C(2C+1)\begin{pmatrix}A&B&C\\a&b&c\end{pmatrix}\begin{pmatrix}A&B&C\\a'&b'&c'\end{pmatrix}D^{C*}_{cc'}(\alpha,\beta,\gamma) \tag{A.8}$$

we find:

$$D^{\frac{1}{2}}_{s_1'-s_2}(R)D^{\frac{1}{2}}_{-s_2's_1}(R) = 3\begin{pmatrix} \frac{1}{2} & \frac{1}{2} & 1 \\ s_1' & -s_2' & s_2'-s_1' \end{pmatrix}\begin{pmatrix} \frac{1}{2} & \frac{1}{2} & 1 \\ -s_2 & s_1 & s_2-s_1 \end{pmatrix} D^{1*}_{s_2'-s_1',s_2-s_1}(R) + \begin{pmatrix} \frac{1}{2} & \frac{1}{2} & 0 \\ s_1' & -s_2' & s_2'-s_1' \end{pmatrix}\begin{pmatrix} \frac{1}{2} & \frac{1}{2} & 0 \\ -s_2 & s_1 & s_2-s_1 \end{pmatrix} D^{0*}_{s_2'-s_1',s_2-s_1}(R) \tag{A.9}$$

where s_1', s_2', s_1, s_2 can take values of $\pm\frac{1}{2}$. The $D^{0*}_{s_2'-s_1',s_2-s_1}(R)$ part doesn't contribute either, because it also requires $s_1' = s_2', s_1 = s_2$, which makes it vanish when to sum over $\mathbf{p}$.

It follows from the second equality of (A.4) that

$$D^1_{m_1m_2}(R) = \sum_m D^{1*}_{mm_1}(\varphi', \theta', -\varphi')D^1_{mm_2}(\varphi, \theta, -\varphi) \tag{A.10}$$

and we arrive at

$$A_{s_1',s_2';s_1,s_2}(\mathbf{p}', \mathbf{p}) = 12(-1)^{s_2+s_2'-1}C_{s_1'-s_2'}(p')C_{s_1-s_2}(p)e^{i(-\theta_{\mathbf{p}s_2}+\theta_{\mathbf{p}'s_2'})}\begin{pmatrix} \frac{1}{2} & \frac{1}{2} & 1 \\ s_1' & -s_2' & s_2'-s_1' \end{pmatrix}\begin{pmatrix} \frac{1}{2} & \frac{1}{2} & 1 \\ -s_2 & s_1 & s_2-s_1 \end{pmatrix} \times \sum_m D^1_{m,s_2'-s_1'}(R)D^1_{m,s_2-s_1}(R) + ... \tag{A.11}$$

with "..." the terms not contributing to the summation over momenta.

Substituting (A.11) into (2.11), the interaction term of (2.11) becomes

$$\sum_{\mathbf{p},\mathbf{p}',\mathbf{s_1'},\mathbf{s_2'},\mathbf{s_1},\mathbf{s_2}} A_{s_1',s_2';s_1,s_2}(\mathbf{p}', \mathbf{p})a^\dagger_{\mathbf{p}',s_1'}\varepsilon^c\tilde{a}^\dagger_{-\mathbf{p}',s_2'}\tilde{a}_{-\mathbf{p},s_2}\varepsilon^c a_{\mathbf{p},s_1} = 12\sum_{\mathbf{p},\mathbf{p}'}\Xi^{\nu\dagger}_\mu(\mathbf{p}')\Xi^\nu_\mu(\mathbf{p}) \tag{A.12}$$

with

$$\Xi^\nu_\mu(\mathbf{p}) = \sum_{s_1,s_2}(-1)^{s_2-\frac{1}{2}}e^{-i\theta_{\mathbf{p}s_2}}C_{s_1-s_2}(p)\begin{pmatrix} \frac{1}{2} & \frac{1}{2} & 1 \\ -s_2 & s_1 & s_2-s_1 \end{pmatrix} D^{1\ *}_{\mu,s_2-s_1}(\varphi, \theta, -\varphi)\tilde{a}_{-\mathbf{p}s_2}J^\nu a_{\mathbf{p}s_1} \tag{A.13}$$

If follows from the explicit form of the phase factor (2.20) and the symmetry properties of the D-functions that

$$\Xi^\nu_\mu(-\mathbf{p}) = \sum_{s_1,s_2}(-1)^{s_2-\frac{1}{2}}e^{-i\theta_{\mathbf{p}s_2}}C_{-s_1s_2}(p)\begin{pmatrix} \frac{1}{2} & \frac{1}{2} & 1 \\ -s_2 & s_1 & s_2-s_1 \end{pmatrix} D^{1\ *}_{\mu,s_2-s_1}(\varphi, \theta, -\varphi)\tilde{a}_{-\mathbf{p}s_2}J^\nu a_{\mathbf{p}s_1} \tag{A.14}$$

On writing $\sum'_{\mathbf{p},\mathbf{p}'}\Xi^{\nu\dagger}_\mu(\mathbf{p})$ with the summation $\sum'$ extending half space of and we end up with (2.18) with

$$\Phi^\nu_\mu(\mathbf{p}) \equiv \Xi^\nu_\mu(\mathbf{p}) + \Xi^\nu_\mu(-\mathbf{p}) \tag{A.15}$$

given by (2.19).

Appendix B

In this section, we will give the details of the diagonalization procedure of the 6×6 matrix $MM^\dagger$ for each single flavor phase. We shall write $MM^\dagger \equiv \Delta^2\mathcal{M}$. The eigenvalues of $\mathcal{M}$ corresponds to $f^2(\theta)$ shown in (3.13).

The polar phase:

It's straightforward to show

$$\mathcal{M}_{\text{polar}} = \frac{3}{2}\begin{pmatrix} (\sin^2\theta + \lambda^2\cos^2\theta)J_0^2 & 0 \\ 0 & (sin^2\theta + \lambda^2\cos^2\theta)J_0^2 \end{pmatrix} \tag{B.1}$$

and the color operator J_0^2 decouples. The eigenvalues of J_0^2 are $1, 1, 0$ and the functional forms of $f(\theta)$ are therefore given by the 3rd line of (3.13).

The A phase:

In this case we have

$$\mathcal{M}_{\rm A} = 3\begin{pmatrix} (2\sin^4\frac{\theta}{2}+\frac{1}{2}\lambda^2\sin^2\theta)J_0^2 & -\lambda\sin\theta e^{i\varphi}J_0^2 \\ -\lambda\sin\theta e^{i\varphi}J_0^2 & (2\cos^4\frac{\theta}{2}+\frac{1}{2}\lambda^2\sin^2\theta)J_0^2 \end{pmatrix} \tag{B.2}$$

The color operator J_0^2, which has eigenvalues 1,1 and 0, decouples again. The forms of $f(\theta)$ given by the fourth line of (3.13) correspond to the eigenvalues of the 2×2 matrix obtained from (B.2) by replacing J_0^2 with its eigenvalues.
The planar phase:

The diagonalization of $MM^\dagger$ is less straightforward because of the coupling between the helicity and the color indexes. In terms of $J'_\pm \equiv J_\pm e^{\mp i\varphi}$, we have

$$\mathcal{M}_{\rm Planar} = \frac{3}{4}\begin{pmatrix} a & b \\ c & d \end{pmatrix} \tag{B.3}$$

where:

$$a = \left(\cos^4\frac{\theta}{2}+\frac{1}{4}\lambda^2\sin^2\theta\right)J'_-J'_+ + \left(\sin^4\frac{\theta}{2}+\frac{1}{4}\lambda^2\sin^2\theta\right)J'_+J'_- - \frac{1}{4}(1-\lambda^2)(J'^2_- + J'^2_+)\sin^2\theta \tag{B.4a}$$

$$b = \frac{\lambda}{2}\sin\theta e^{-i\varphi}[J'_+, J'_-] \qquad c = b^\dagger \tag{B.4b}$$

$$d = \left(\sin^4\frac{\theta}{2}+\frac{1}{4}\lambda^2\sin^2\frac{\theta}{2}\right)J'_-J'_+ + \left(\cos^4\frac{\theta}{2}+\frac{1}{4}\lambda^2\sin^2\theta\right)J'_+J'_- - \frac{1}{4}(1-\lambda^2)(J'^2_- + J'^2_+)\sin^2\theta \tag{B.4c}$$

Since $J'_\pm \equiv J_\pm e^{\mp i\varphi}$ and J_0 satisfy the same angular momentum algebra as $J_\pm$ and J_0 do, we shall work in the representation where

$$J'_+ = \sqrt{2}\begin{pmatrix} 0 & 1 & 0 \\ 0 & 0 & 1 \\ 0 & 0 & 0 \end{pmatrix} \qquad J'_- = \sqrt{2}\begin{pmatrix} 0 & 0 & 0 \\ 1 & 0 & 0 \\ 0 & 1 & 0 \end{pmatrix}. \tag{B.5}$$

and $J_0 = \mathrm{diag}(1,0,-1)$. It follows that

$$a = \begin{pmatrix} 2\sin^4\frac{\theta}{2}+\frac{\lambda^2}{2}\sin^2\theta & 0 & \frac{1}{2}(1-\lambda^2)\sin^2\theta \\ 0 & 1+\cos^2\theta+\lambda^2\sin^2\theta & 0 \\ \frac{1}{2}(1-\lambda^2)\sin^2\theta & 0 & 2\cos^4\frac{\theta}{2}+\frac{\lambda^2}{2}\sin^2\theta \end{pmatrix} \tag{B.6a}$$

$$b = \lambda\sin\theta e^{-i\varphi}\begin{pmatrix} 1 & 0 & 0 \\ 0 & 0 & 0 \\ 0 & 0 & -1 \end{pmatrix} \tag{B.6b}$$

$$d = \begin{pmatrix} 2\cos^4\frac{\theta}{2}+\frac{\lambda^2}{2}\sin^2\theta & 0 & \frac{1}{2}(1-\lambda^2)\sin^2\theta \\ 0 & 1+\cos^2\theta+\lambda^2\sin^2\theta & 0 \\ \frac{1}{2}(1-\lambda^2)\sin^2\theta & 0 & 2\sin^4\frac{\theta}{2}+\frac{\lambda^2}{2}\sin^2\theta \end{pmatrix} \tag{B.6c}$$

By permutations of the rows and columns, this 6 by 6 matrix is transformed into the block-diagonal form

$$\mathcal{M}_{\rm Planar} = \begin{pmatrix} 1+\cos^2\theta+\lambda^2\sin^2\theta & 0 & 0 \\ 0 & 1+\cos^2\theta+\lambda^2\sin^2\theta & 0 \\ 0 & 0 & M_4 \end{pmatrix} \tag{B.7}$$

where M_4 is a 4 by 4 matrix, given by

$$M_4 = \begin{pmatrix} 2\sin^4\frac{\theta}{2}+\frac{\lambda^2}{2}\sin^2\theta & \frac{1}{2}(1-\lambda^2)\sin^2\theta & \lambda\sin\theta e^{-i\varphi} & 0 \\ \frac{1}{2}(1-\lambda^2)\sin^2\theta & 2\cos^4\frac{\theta}{2}+\frac{\lambda^2}{2}\sin^2\theta & 0 & -\lambda\sin\theta e^{-i\varphi} \\ \lambda\sin\theta e^{i\varphi} & 0 & 2\cos^4\frac{\theta}{2}+\frac{\lambda^2}{2}\sin^2\theta & \frac{1}{2}(1-\lambda^2)\sin^2\theta \\ 0 & \lambda\sin\theta e^{i\varphi} & \frac{1}{2}(1-\lambda^2)\sin^2\theta & 2\sin^4\frac{\theta}{2}+\frac{\lambda^2}{2}\sin^2\theta \end{pmatrix} \tag{B.8}$$

It is straightforward to show that the secular equation

$$\det(M_4 - z) = z^2(z - 1 - \cos^2\theta - \lambda^2 \sin^2\theta)^2 \tag{B.9}$$

which, together with (B.7), yield the eigenvalues in the second line of (3.13).

The CSL phase:

In terms of the operator $\mathcal{J}_\pm$ and $\mathcal{J}_0$, the matrix $\mathcal{M}$ of CSL takes the form

$$\mathcal{M}_{\rm CSL} = \frac{1}{2}\begin{pmatrix} \mathcal{J}_-\mathcal{J}_+ + \lambda^2\mathcal{J}_0^2 & \lambda e^{-i\varphi}[\mathcal{J}_0, \mathcal{J}_-] \\ -\lambda e^{i\varphi}[\mathcal{J}_0, \mathcal{J}_+] & \mathcal{J}_+\mathcal{J}_- + \lambda^2\mathcal{J}_0^2 \end{pmatrix} \tag{B.10}$$

The operators $\mathcal{J}_\pm$ and $\mathcal{J}_0$ satisfy the same algebraic relations as $J_\pm$ and J_0, such as $[\mathcal{J}_0, \mathcal{J}_\pm] = \pm\mathcal{J}_\pm$. In the representation where $\mathcal{J}_0$ is diagonal, i.e. $\mathcal{J}_0 = \text{diag.}(1, 0, -1)$,

$$\mathcal{J}_+ = \sqrt{2}\begin{pmatrix} 0 & 1 & 0 \\ 0 & 0 & 1 \\ 0 & 0 & 0 \end{pmatrix} \text{ and } \mathcal{J}_- = \sqrt{2}\begin{pmatrix} 0 & 0 & 0 \\ 1 & 0 & 0 \\ 0 & 1 & 0 \end{pmatrix} \tag{B.11}$$

we have $\mathcal{J}_-\mathcal{J}_+ = \text{diag}(0, 2, 2)$, $\mathcal{J}_+\mathcal{J}_- = \text{diag}(2, 2, 0)$. Substituting these into (B.10), we find that

$$\mathcal{M}_{\rm CSL} = \frac{1}{2}\begin{pmatrix} \lambda^2 & 0 & 0 & 0 & 0 & 0 \\ 0 & 2 & 0 & -\sqrt{2}\lambda e^{-i\varphi} & 0 & 0 \\ 0 & 0 & 2+\lambda^2 & 0 & -\sqrt{2}e^{-i\varphi} & 0 \\ 0 & -\sqrt{2}\lambda e^{i\varphi} & 0 & 2+\lambda^2 & 0 & 0 \\ 0 & 0 & -\sqrt{2}\lambda e^{i\varphi} & 0 & 2 & 0 \\ 0 & 0 & 0 & 0 & 0 & \lambda^2 \end{pmatrix} \tag{B.12}$$

By permutations of the rows and columns, this 6 by 6 matrix is transformed into the block-diagonal form

$$\frac{1}{2}\begin{pmatrix} \lambda^2 & 0 & 0 & 0 & 0 & 0 \\ 0 & \lambda^2 & 0 & 0 & 0 & 0 \\ 0 & 0 & 2 & -\sqrt{2}\lambda e^{-i\varphi} & 0 & 0 \\ 0 & 0 & -\sqrt{2}\lambda e^{i\varphi} & 2+\lambda^2 & 0 & 0 \\ 0 & 0 & 0 & 0 & 2+\lambda^2 & -\sqrt{2}\lambda e^{-i\varphi} \\ 0 & 0 & 0 & 0 & -\sqrt{2}\lambda e^{i\varphi} & 2 \end{pmatrix} \tag{B.13}$$

and the eigenvalues in the first line of (3.13) follow then.

---

[1] M. G. Alford, A. Schmitt, K, Rajagopal and T. Schäfer, Rev. Mod. Phys. 80:1455-1515, 2008 and the references therein.
[2] M. Alford, J. Berges and K. Rajagopal, Nucl. Phys. B**558**, 219 (1999).
[3] T. Schäfer and F. Wilczek, Phys. Rev. D**60**, 074014 (1999).
[4] T. Schäfer, Nucl. Phys. B**575**, 269-284 (2000).
[5] R. D. Pisarski, Phys. Rev. C**62** 035202 (2000).
[6] M. Alford, K. Rajagopal and F. Wilczek, Nucl. Phys. B**537**, 443 (1999).
[7] Mei Huang, Peng-fei Zhuang, Wei-qin Chao, Phys. Rev. D**67**, 065015 (2003); Mei Huang, Igor A. Shovkovy, Phys. Lett. B**564**, 205 (2003).
[8] M. Alford, C. Kouvaris and K. Rajagopal, Phys. Rev. Lett. **92**, 222001 (2004); M. Alford, J. Bowers and K. Rajagopal, Phys. Rev. D**63**, 074016 (2001).
[9] M. Huang and I. Shovkovy, Phys. Rev. D**70**, 051501(R) (2004); K. Fukushima, Phys. Rev. D**72**, 074002 (2005).
[10] T. Schäfer, Phys. Rev. D**62**, 094007 (2000).
[11] A. Schmitt, Q. Wang and D. H. Rischke, Phys. Rev. Lett. **91**, 242301 (2003).
[12] Andreas Schmitt, Phys. Rev. D**71**, 054016 (2005).
[13] C. Thompson and R. C. Duncan, Astrophys. J. 473, 322 (1996).
[14] Bo Feng, De-fu Hou, Hai-cang Ren, and Ping-ping Wu, Phys. Rev. Lett. **105**, 042001 (2010).
[15] S. B. Ruester, V. Werth, M. Buballa, I. A. Shovkovy and D. H. Rischke, Phys. Rev. D**72**, 034004 (2005).
[16] D. N. Aguilera, D. Blaschke, M. Buballa and V. L. Yudichev, Phys. Rev. D**72**, 034008 (2005).
[17] D. T. Son, Phys. Rev. D**59**, 094019 (1999); T. Schäfer and F. Wilczek, Phys. Rev. D**60**, 114033 (1999); R. D. Pisarski and D. H. Rischke, Phys. Rev. D**61**, 074017 (2000); D. K. Hong, V. A. Miransky, I. A. Shovkovy and C. R. Wijewardhana, Phys. Rev. D**61**, 056001 (2000); W. E. Brown, J. T. Liu and H-C Ren, Phys. Rev. D**61**, 114012 (2000); Phys. Rev. D**62**, 054016 (2000).

[18] D. T. Son, M. A. Stephanov, Phys. Rev. D**77**, 014021 (2008).
[19] Sh. Fayazbakhsh, N. Sadooghi, Phys. Rev. D**83**, 025026 (2011).
[20] E. J. Ferrer, V. de la Incera, Jason P. Keith, Israel Portillo, Paul L. Springsteen, Phys. Rev. C**82**, 065802 (2010).
[21] E. J. Ferrer, V. de la Incera and C. Manuel, Phys. Rev. Lett. **95**, 152002 (2005); Nucl. Phys. B**747**, 88 (2006); Bo Feng, E. J. Ferrer and V. de la Incera, arXiv:1105.2498.
[22] Ping-ping Wu, Hang He, De-fu Hou, and Hai-cang Ren, Phys. Rev. D**84**, 027701 (2011).
[23] J. Noronha and I. A. Shovkovy, Phys. Rev. D**76**, 105030 (2007).
[24] K. Fukushima and H. Warringa, Phys. Rev. Lett. **100**, 032007 (2008).
[25] T. Brauner, Phys. Rev. D**78**, 125027 (2008); Jin-yi Pang, Tomas Brauner and Qun Wang, Nucl. Phys. A**852**, 175 (2011).